Structural Changes at Synapses After Delayed Perfusion Fixation in Different Regions of the Mouse Brain

JUNG-HWA TAO-CHENG,[1] PAUL E. GALLANT,[2] MILTON W. BRIGHTMAN,[2] AYSE DOSEMECI,[2] AND THOMAS S. REESE[2]*

[1]EM Facility, National Institute of Neurological Disorders and Stroke, National Institutes of Health, Bethesda, Maryland 20892

[2]Laboratory of Neurobiology, National Institute of Neurological Disorders and Stroke, National Institutes of Health, Bethesda, Maryland 20892

ABSTRACT

We recently showed by electron microscopy that the postsynaptic density (PSD) from hippocampal cultures undergoes rapid structural changes after ischemia-like conditions. Here we report that similar structural changes occur after delay in transcardial perfusion fixation of the mouse brain. Delay in perfusion fixation, a condition that mimics ischemic stress, resulted in 70%, 90%, and 23% increases in the thickness of PSDs from the hippocampus (CA1), cerebral cortex (layer III), and cerebellar cortex (Purkinje spines), respectively. In step with PSD thickening, the amount of PSD-associated α-calcium calmodulin-dependent protein kinase II (α- CaMKII) label increased more in cerebral cortical spines than in Purkinje spines. Although the Purkinje PSDs thickened only slightly after delayed fixation, they became highly curved, and many formed sub-PSD spheres ~80 nm in diameter that labeled for CaMKII. Delayed perfusion fixation also produced more cytoplamic CaMKII clusters (~110 nm in diameter) in the somas of pyramidal cells (from hippocampus and cerebral cortex) than in Purkinje cells. Thus a short delay in perfusion fixation produces cell-specific structural changes at PSDs and neuronal somas. Purkinje cells respond somewhat differently to delayed perfusion fixation, perhaps owing to their lower levels of CaMKII, and CaMKII binding proteins at PSDs. We present here a catalogue of structural changes that signal a perfusion fixation delay, thereby providing criteria by which to assess perfusion fixation quality in experimental structural studies of brain and to shed light on the subtle changes that occur in intact brain following metabolic stress. J. Comp. Neurol. 501:731–740, 2007. Published 2007 Wiley-Liss, Inc.[†]

Indexing terms: PSD thickness; PSD curvature; CaMKII; cerebellum; hippocampus; cerebral cortex

The postsynaptic density (PSD) from asymmetric glutamatergic synapses in mammals is a dense layer lying beneath the postsynaptic membrane (for review see Peters and Palay, 1996). Previously, we showed in dissociated hippocampal cultures that PSDs rapidly thicken after depolarization by high K^+ as well as treatment with glutamate or N-methyl-D-aspartate (NMDA; Dosemeci et al., 2001, 2002). PSD thickening is accompanied by an increase in calcium calmodulin-dependent protein kinase II (CaMKII) immunolabel at the PSD. Translocation of CaMKII to the PSD is at least partially responsible for the increase in PSD thickness (Dosemeci et al., 2002; Chen et al., 2005). Transient cerebral ischemia (Martone et al., 1999) and metabolic uncoupling that mimics ischemia (Dosemeci et al., 2000) also induced similar PSD thickenings.

The realization that the PSD is a dynamic structure that can become modified within minutes necessitates

Grant sponsor: Intramural Research Program of the National Institute of Neurological Disorders and Stroke, National Institutes of Health.

*Correspondence to: Tom Reese, NIH, Bldg. 49, Room 3A60, Bethesda, MD 20892. E-mail: treese@mbl.edu

Received 29 June 2006; Revised 2 October 2006; Accepted 28 November 2006

DOI 10.1002/cne.21276

Published online in Wiley InterScience (www.interscience.wiley.com).

new scrutiny of the conditions used to fix brains by perfusion, a procedure that can take several minutes to complete (Palay et al., 1962). One step of transcardial perfusion fixation that could be especially crucial is the interval between the cessation of breathing and the introduction of fixatives to replace blood. This interval represents a virtual ischemic episode, which could induce structural changes at the PSD. This period of ischemia-like stress is further prolonged when saline is introduced to flush out the blood or if the fixative does not reach the tissues quickly as a result of technical failures.

We have previously demonstrated that a 5–10-minute delay in perfusion fixation caused formation of "CaMKII clusters," aggregates of CaMKII molecules ~110 nm in diameter, in CA1 pyramidal somas in rat hippocampus (Tao-Cheng et al., 2001). Such cytoplasmic CaMKII clusters are also formed in dissociated hippocampal neurons in culture under ischemia-like stress, accompanied by a marked increase in PSD-associated CaMKII (Dosemeci et al., 2000). Because self-association of α-CaMKII may be a key event in both PSD thickening and cytoplasmic CaMKII clustering (Hudmon et al., 2005), we also looked to see whether there is a correlation between these structural changes and the concentration of α-CaMKII in neurons from different parts of the brain. We compare the hippocampus, the cerebral cortex, and the cerebellum, a comparison based on previous reports showing a much higher α-CaMKII content in the forebrain (which includes the hippocampus and the cerebral cortex) than in the cerebellum (Erondu and Kennedy, 1985; Walaas et al., 1988).

The present study compares the effects of a specified perfusion fixation delay (5–8 minutes) on neurons from different regions of the mouse brain. Most early EM documentation of synaptic structures was performed on perfusion-fixed rat brains, but the need to examine the mouse brain has increased in recent years with the generation of knockout and transgenic mice with altered synaptic proteins. The present study will help to identify artifacts of perfusion fixation and introduce new guidelines for structural analysis of PSD and neuronal soma obtained from perfusion-fixed brains. Furthermore, distinct responses in different neuronal types may shed light on the mechanisms of PSD thickening and CaMKII redistribution under ischemic stress.

MATERIALS AND METHODS

Anesthesia

The animal protocol used in this study was approved by the NIH Animal Use and Care Committee and conforms to NIH guidelines. C57 black and NIH Swiss adult male mice (DCT, NIH), 25–35 g in weight, were used for all experiments. Data were collected from four fast-fixed and five delay-fixed mice. Each fast-fixed mouse was paired with at least one delay-fixed mouse taken from the same litter and fixed on the same day. Each mouse was initially anesthetized in a plastic flow chamber with 5% isoflurane carried by 100% oxygen. After the mouse was unresponsive to toe pinch, it was moved to a perfusion station inside a chemical fume hood. Anesthesia was maintained by delivering 2% isoflurane in oxygen through a facemask.

Surgical procedures

To avoid accidental movement during the surgery and perfusion, the anesthetized mouse was pinned down, through the forelimb and hind limb skin, onto a 1–2-cm-thick soft-vinyl dissecting pad. The abdominal cavity was then opened with a long scissor cut through the abdominal wall. This first cut was placed parallel and close to the caudal end of the rib cage. This cut exposed the diaphragm and ribs from below. A cut was then made through the diaphragm and lateral aspect of the rib cage parallel to the spinal column and close to the supporting vinyl dissecting pad. The timer was started when the diaphragm was first cut, because this halted air exchange in the lungs. A cut was then made to separate the diaphragm from the rib cage wall. Cutting the second side of the rib cage, close to the lateral angle of each rib and parallel to the spinal column, completed the rib flap. This exposure left a shallow chest cavity to be easily drained of welling blood so that the heart would remain visually exposed during the whole cannulation and perfusion procedure. A hemostat (Roboz RS 7130 or Vantage 97-36) was carefully placed on the rib flap so that the major chest wall arteries, especially the internal thoracic arteries were clamped to prevent them from stealing flow during the perfusion. The rib cage flap was then reflected toward the head to expose the heart. The rib cage flap was held in place by pinning the locked hemostat to the vinyl pad.

A pair of broad-toothed dissecting forceps (Roboz RS 8247 or Vantage V6-8) was then used to retract the heart gently, without cutting or damaging it. The right atrium was then cut with small scissors followed immediately by a small cut made into the left ventricle close to its apex. A size 18 or 20 cannula that had been blunted and polished to a smooth elliptical opening (to decrease the possibility of tearing the heart tissue and to increase the flow rate) was inserted into the opening of the ventricle, but not into the aorta, because this might have damaged the aorta. To prevent leakage of blood around the cannula, the cannula was manually held in place with the same dissecting forceps used to hold the heart. The exact pressure that was needed to prevent leakage around the cannula without tearing the heart was then maintained by rapidly and gently clamping the distal end of these forceps with a hemostat. To adjust the pressure on the forceps to the proper level, the hemostat closure tension and the exact clamping position of the hemostat along the forceps were adjusted. The locked hemostat was then pinned in place, taking care not to twist the heart vessels or to otherwise block the flow of the perfusate.

Perfusion and fixation procedures

Perfusates were typically delivered by gravity flow at a hydrostatic pressure of about 5 feet. For "fast perfusion fixation" the total lapsed time was counted from the first cut of the diaphragm to the time when a visible outflow of perfusate (fixative) from the atrium was noted. We accepted only animals that were successfully perfused within 100 seconds (samples used in this study were from 55 to 95 seconds). Within this time restriction, for acceptance as a usable perfusion, the liver had to be cleared of blood, and the exposed skin of the ears and nose had to have turned white. Unless noted, perfusion solutions were maintained at room temperature. For "delayed perfusion fixation," blood was flushed out for 5–8 minutes with

phosphate-buffered saline (PBS; containing 1 mM Ca^{2+} and 0.5 mM Mg^{2+}) before fixative was introduced. Brains were prepared for standard electron microscopy (EM) or immuno-EM.

For standard EM, a mixture of 2% gluteraldehyde and 2% paraformaldehyde in 0.1 N sodium cacodylate buffer at pH7.4 was used as the initial fixative. One set of animals was perfused with warm perfusates at 37°C. No apparent improvements were detected between these samples and those that were perfused with room-temperature perfusates, so room temperature perfusates were used in all other animals. After perfusion fixation, brains were left in situ overnight, dissected the next day, vibratome-sectioned into 100 μm slices, and further immersion fixed in 4% glutaraldehyde from overnight to 2 weeks. Slices were treated with 1% OsO_4 in cacodylate buffer for 1 hour on ice and 0.25% uranyl acetate in acetate buffer at pH 5.0 overnight at 4°C, dehydrated with ethanol and propylene oxide, and flat embedded in epoxy resin between two plastic slides.

For immuno-EM, 1 minute of perfusion with 6–10 ml of 3.5% acrolein and 2% paraformaldehyde in 0.1 M phosphate buffer at pH 7.4, or 3.5% acrolein alone in phosphate buffer was followed by 5–15 minutes of perfusion with 50 ml 2% paraformaldehyde (for review of acrolein perfusion fixation see Sesack et al., 2006). For safety concerns, fixative was delivered with a syringe when using acrolein. Brains for immuno-EM were dissected and examined as soon as perfusion fixation was finished. If the brains were soft, or pink they were discarded. Only hardened brains cleared of blood were accepted and further fixed by immersion in 2% paraformaldehyde for a total of 60 minutes of fixation (counted from the start of perfusion fixation). Some brain slices fixed for immuno-EM were also further immersion fixed in 4% glutaraldehyde and processed for standard EM.

Preembedding EM immunogold procedures

Characterization of antibodies. Mouse monoclonal antibody against α-CaMKII (clone 6G9-2 from Chemicon, Temecula, CA; catalog No. MAB8699; originally prepared using the purified CaMKII by Erondu and Kennedy, 1985) was used at 1:100 dilution (10 μg/ml). On Western blots of mouse brain tissue, it recognizes a single band at approximately 55 kDa (Stephan Miller, unpublished data; Silva et al., 1992), and no band is observed in Westerns from α-CaMKII knockout mice (Silva et al., 1992). The antibody has been widely used to study the distribution of α-CaMKII in a variety of preparations from rat and mice (Erondu and Kennedy, 1985; Dosemeci et al., 2000; Miller et al., 2002). Additional controls for α-CaMKII immunolabeling included omitting the primary antibody.

Immunolabeling procedures. As previously described (Tao-Cheng et al., 2001), all steps were carried out at room temperature unless otherwise indicated. Briefly, vibratomed slices were washed in PBS, blocked and made permeable with 5% normal goat serum and 0.1% saponin in PBS for 1 hour, treated with mouse monoclonal antibody against α-CaMKII for 1–2 hours, washed and treated with secondary antibody conjugated with 1.4-nm gold particles (Nanogold, 1:250; Nanoprobes, Yaphand, NY) for 1 hour, and silver enhanced for 10–20 minutes with the HQ kit from Nanoprobes. Slices were then treated with 0.2% OsO_4 in phosphate buffer for 30 minutes, mordanted en bloc with 0.25% uranyl acetate overnight at 4°C, dehydrated with ethanol, and flat embedded in epoxy resin. Thin sections were counterstained with uranyl acetate and lead citrate.

Morphometry

Sampling. Flat-embedded brain slices were examined under the light microscope to identify regions of the brain. Cerebral cortical synapses were sampled from layer III (traced from the meninges to the first layer showing a high density of pyramidal neuronal somas) of cortex above the hippocampus. Cerebellar synapses were sampled from the outer molecular layer where virtually all synapses are made by parallel fibers of granular cells with Purkinje cell spines (Gundappa-Sulur et al., 1999). The zonula radiata of the CA1 region of the hippocampus was identified, and synapses were sampled from areas proximal to the edge of the clustered pyramidal cell somas. In randomly chosen grid openings from selected areas, every cross-sectioned synapse encountered was photographed with a CCD digital camera system (XR-100 from AMT, Danvers, MA) at ×40,000 and printed at a final magnification of ×150,000 for PSD measurement. Prints for measurements from different groups of samples were printed on the same printer on the same day, then mixed and measured blind without individual adjustment for brightness or contrast. All measurements of PSD thickness and curvature were made from the same set of synapses. Only images in publication plates were adjusted for brightness and contrast in Adobe Photoshop.

Measurement of PSD thickness and curvature. Measurement of PSD thickness was as previously described (Dosemeci et al., 2001). Briefly, the outline of the PSDs were traced and then divided by the PSD length. The curvature of a PSD is expressed as the height of its arc above a chord drawn between its ends, then converted to a percentage. A curvature of zero denotes a flat PSD, which does not arc up or down. Micrographs for measurement were oriented so that presynaptic terminals were consistently situated at the top of the PSD. PSDs that arch up into the presynaptic terminal are given positive percentage values, whereas those with negative values arch down into the postsynaptic spine.

In the present study, based on single sections, each cross-sectioned PSD was counted as one entity, and no distinction was made between macular and perforated PSD. For example, a perforated PSD would have been counted as two separated PSDs if both were cross-sectioned with distinct membranes. It should be noted that, consistently with a previous 3D analysis (Spacek and Harris, 1997), the great majority of the PSD analyzed in forebrain spines were macular.

Presence of spine apparatus. The criteria for identifying "spine apparatus" was according to the original description by Gray (1959; for review see Peters et al., 1991): a few membrane-bound cisternae alternating with laminae of dense materials. Micrographs of the particular brain regions were taken and printed at a final magnification of ×37,500. The presence or absence of spine apparatus was scored for every spine.

Measurement of α-CaMKII labeling, CaMKII cluster concentrations, and PSD-associated α-CaMKII labeling. Areas of neuronal soma cytoplasm (excluding nucleus) and spines were measured in NIH Image. Individual silver-enhanced signals and cytoplasmic CaMKII clusters (aggregates of CaMKII molecules of ~110 nm in average diameter) were counted and divided by the areas. PSD-associated

α-CaMKII labeling was measured by counting all grains within and touching the outlined PSD. For each spine, the number of PSD-associated silver grains was divided by the total number of grains within that spine, to yield percentage of α-CaMKII labeling associated with the PSD. Statistical analysis (KaleidaGraph by Synergy Software) was carried out by Student's *t*-test (two-sided, unpaired data with unequal variance) with confidence level set at $P < 0.01$ unless otherwise indicated.

RESULTS

Quality of perfusion fixation

The quality of perfusion-fixed brain samples depends on the continuous flow of oxygenated blood prior to fixation and the subsequent perfusion of fixative with a good flow rate to replace the blood rapidly and completely throughout the brain. Our criteria for a good perfusion fixation based on gross inspection of the fixed brain are the absence of blood-filled vessels, uniformity of color change resulting from the fixative replacing the blood, and uniformity of hardening resulting from the chemical reaction by the fixatives.

The final assessment of cell preservation can be made only by EM. Poor fixation resulting from inadequate perfusion is evident from extended extracellular spaces, swelling of mitochondria, and selective swelling of dendrites and astrocytic lamellas (Palay et al., 1962; Karlsson and Schultz, 1966). In the present study, any brains showing signs of poor blood flow or poor fixation were discarded to ensure that the fast-perfusion (<100 seconds delay, Fig. 1A,C) and delayed-perfusion (5–8 minutes delay, Fig. 1B,D) fixation experiments actually represented the

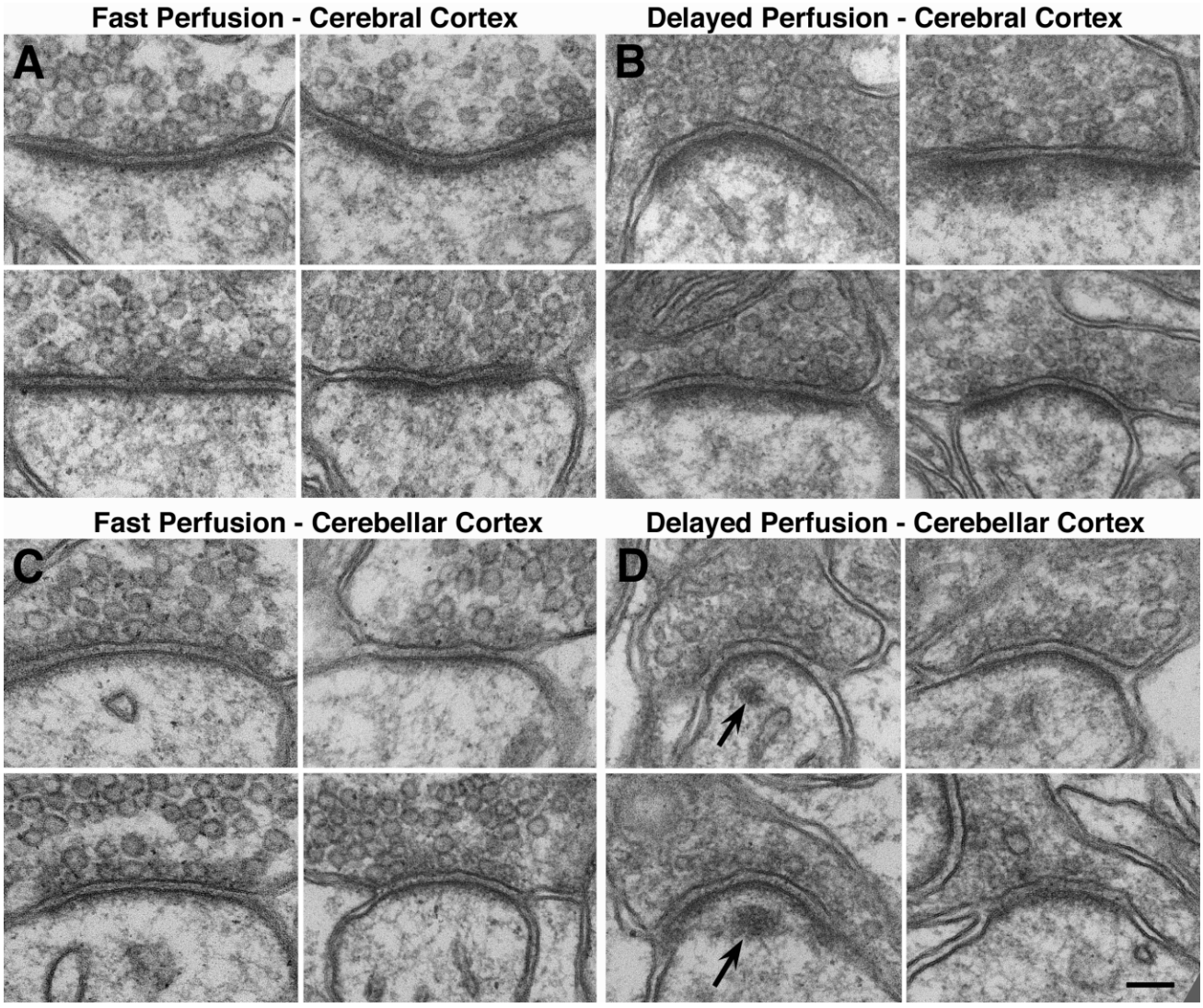

Fig. 1. **A–D:** Structural changes in postsynaptic densities (PSDs) after delayed perfusion fixation. Presynaptic terminal is situated at the top of each panel. PSD thickness increases significantly in cerebral cortex (B vs. A) but only slightly in cerebellar cortex (D vs. C). Arrows in D indicate sub-PSD spheres present in cerebellar spines after delayed perfusion fixation. Scale bar = 0.1 μm.

stated time points at which the brains were perfusion fixed. Quantitative analyses of changes in PSDs resulting from delayed fixation were thus performed in a selected group of mice for which we are certain that the brains were promptly fixed so that the structural changes actually reflect the stated time delays in perfusion fixation.

Effects of delayed perfusion fixation on thickness and curvature of PSDs

In the fast-perfusion group of brains, cerebral cortical spines (Fig. 1A) had slightly thicker PSDs than the Purkinje spines in cerebellum (Fig. 1C). After delayed fixation, cerebral cortical PSDs increased appreciably in thickness (Fig. 1B), whereas Purkinje spine PSDs from the same mice increased only slightly in thickness (Fig. 1D). Measurements of the average PSD thickness of asymmetric synapses from hippocampus, cerebral cortex, and cerebellar cortex (see Materials and Methods for details on sampling and measurements) showed significant increases in thickness of 70%, 90%, and 23%, respectively (Fig. 2).

After delayed perfusion fixation, the curvature of PSDs increased significantly in both forebrain and Purkinje spines, and always in the direction of becoming more positive (arching into the presynaptic terminal; Figs. 1B,D, 3). This curvature increase was more prominent in Purkinje spines of the cerebellum than in the hippocampus or cerebral cortex (Fig. 3).

The lengths of the PSDs in all three regions were also measured. We noticed that the PSDs in the CA1 zonula radiatum of the hippocampus were shorter than those from the other two regions of the brain ($P < 0.0001$), regardless of the fixation conditions (Fig. 3). Fixation delay did not cause a significant change in the length of the PSD in any of the brain regions studied.

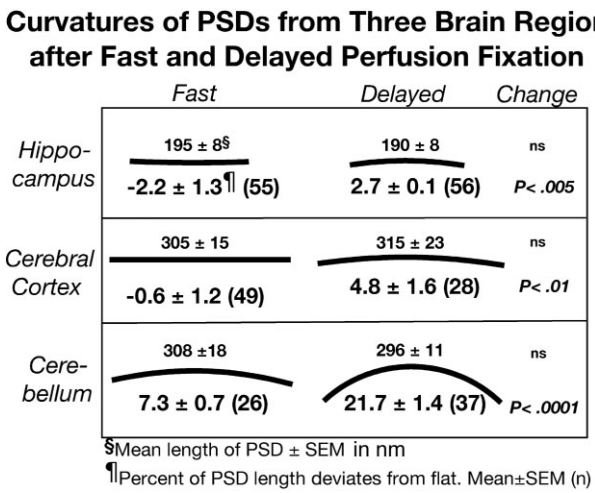

Fig. 3. PSD curvature increases in delayed perfusion fixation. The number at the top of each curve is its length, whereas the number below is its curvature.

Spine apparatus in forebrain synapses is not affected by delay in perfusion

Spine apparatus (Gray, 1959; Fig. 4A,B) was seen only in the forebrain regions, and these were approximately five times more frequent in cerebral cortex than in hippocampus. Consistent with a previous 3D analysis (Spacek and Harris, 1997), spine apparatus was typically found in larger spines (mushroom type). There were no noticeable differences in the fine structure of the spine apparatus in samples fixed rapidly (Fig. 4A) or with a

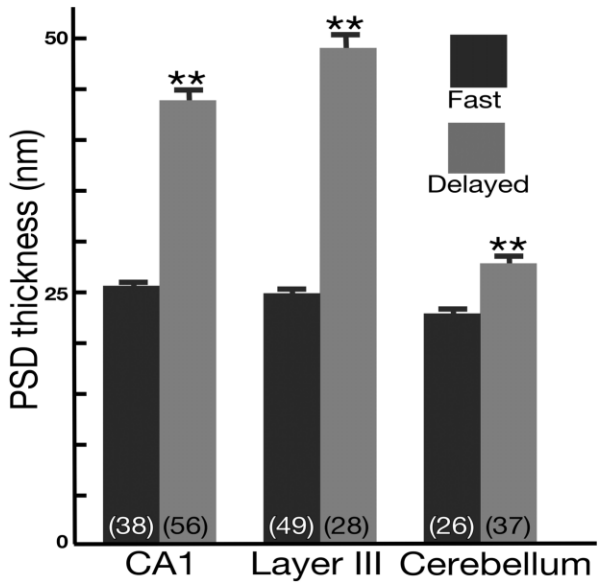

Fig. 2. Average PSD thickness from three regions of the mouse brain after fast and delayed perfusion fixation. PSD thickness significantly (**$P < 0.0001$) increases in all three regions after delayed perfusion fixation. After fast perfusion fixation, cerebellar Purkinje spine PSDs are thinner than those in CA1 region of hippocampus ($P < 0.005$) and layer III of cerebral cortex ($P < 0.001$). Sample size (n) is noted at the base of each bar.

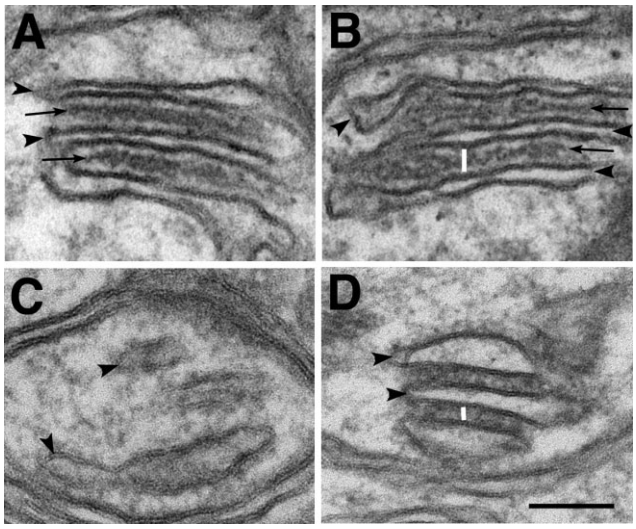

Fig. 4. Spine apparatus from cerebral cortex after fast (**A**) and delayed (**B**) perfusion. Membrane cisternae in the spine apparatus (arrowheads) are separated by an ~35-nm cleft (white bar in B) containing a dense lamina (arrows). Delayed perfusion has no apparent effect on these structures. In contrast, ER-like cisternae (arrowheads in **C,D**) in Purkinje spines are randomly distributed after fast perfusion (C) and become organized into orderly arrays separated by ~20-nm clefts (white bar) after delayed perfusion (D). Scale bar = 0.1 μm.

delay in perfusion fixation (Fig. 4B), nor was the frequency of spine apparatuses affected by delay in perfusion fixation. In the cerebral cortex, 39% (40/103) and 35% (59/167) of spines had spine apparatus after fast and delayed perfusion fixation, respectively. In the hippocampus, the frequencies were 7.5% (12/161) and 8% (23/286) after fast and delayed perfusion fixation, respectively.

No clearcut spine apparatus was seen in cerebellar Purkinje spines, which is consistent with a previous report (Spacek, 1985). In fast-fixed samples, Purkinje spines contained ER-like sacs of smooth membrane in random orientation (arrowheads in Fig. 4C). After delayed perfusion fixation, but never in fast perfusion fixation, 26% (36 of 138 synapses) of the Purkinje spines showed ER stacks in orderly arrays (Fig. 4D). The fine structure of these ER stacks distinguished them from the spine apparatus in forebrain synapses: the spacing between cisternae in Purkinje ER stacks was narrower than that of the forebrain spine apparatus (20 nm vs. 35 nm, respectively). Furthermore, the dense material between the membrane cisternae of the spine apparatus was arranged in a lamina centered in the cleft (arrows in Fig. 4A,B), whereas no such lamina is present between the Purkinje ER stacks (Fig. 4D; for details see Gray, 1959, for spine apparatus, and Takei et al., 1994, for Purkinje ER stacks).

Formation of sub-PSD spheres in Purkinje spines

After delayed fixation, prominent dense structures appeared beneath the PSD (arrows in Fig. 1D) in many of the Purkinje spines. These sub-PSD structures appeared most frequently as a sphere with an average diameter of ~80 nm (Fig. 5A,B) associated with a highly curved PSD. Sub-PSD structures were present in ~45% of Purkinje spines (18 of 39 spines reconstructed from serial sections in one delayed fixed sample). Occasionally, more than one sphere was present per PSD (Fig. 5C), but these multiple spheres were smaller than single ones. Sometimes the sub-PSD structure appeared as a patch of dense material below a relatively flat PSD (Fig. 5D). Radial, filamentous elements (arrowheads in Fig. 5A) spanned the ~35-nm space between sub-PSD structures and the PSD. Possibly the various forms of sub-PSD dense structures represent different stages of sub-PSD sphere formation.

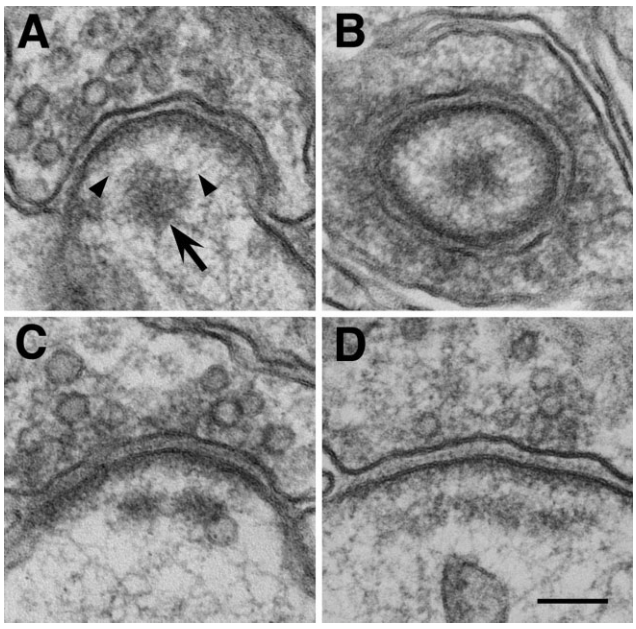

Fig. 5. Structures appear beneath the PSD in Purkinje spines after delayed perfusion fixation. **A:** A single sub-PSD sphere (arrow) connected to the PSD with filamentous material (arrowheads). **B:** A transverse section through a highly curved PSD with a sub-PSD sphere. **C,D:** Different forms of the sub-PSD structure. Scale bar = 0.1 μm.

Sub-PSD spheres were seen in Purkinje spines after delayed- but never in fast-fixed samples (four animals in each group). Similarly, no sub-PSD spheres were ever seen in the forebrain spines in fast-fixed samples. Occasionally, some sub-PSD dense material appeared in forebrain synapses after delayed fixation, but it never assumed a spherical form like the sub-PSD spheres in the Purkinje spines.

α-CaMKII distribution in forebrain neurons and cerebellar Purkinje cells

In fast perfusion fixed brains, labeling for α-CaMKII was mostly dispersed, without aggregation in the soma, dendrites, and dendritic spines of forebrain pyramidal neurons (Fig. 6A for cerebral cortical spine) and the Purkinje cells (Fig. 6D for Purkinje spine). This dispersed pattern was similar to that seen in somas and spines from dissociated hippocampal cultures under unstimulated control conditions (Tao-Cheng et al., 2001; Dosemeci et al., 2001).

Consistent with an earlier light microscopy report (Walaas et al., 1988), Purkinje cells were the only cell type labeled for α-CaMKII in the cerebellum. Our immunogold measurements showed that the concentration of α-CaMKII labeling is higher in cerebral cortical neurons than in Purkinje cells (Fig. 7). The concentration difference between the two cell types was two- to fourfold in neuronal somas and one-and one-half- to twofold in spines. Furthermore, in both cell types, spines had significantly more label than the somas (Fig. 7). The spine to soma labeling ratio was ~4–5 for cerebral cortex and ~6–8 for Purkinje cells.

Redistribution of α-CaMKII in spines after delayed perfusion fixation

After delayed fixation, the bulk of label for α-CaMKII was aggregated at the PSD (Fig. 6B) in the forebrain spines, a pattern similar to that observed in synapses from dissociated hippocampal cultures under ischemia-like stress (Dosemeci et al., 2000). The pattern of redistribution of α-CaMKII in Purkinje spines contrasted with that in forebrain spines. In delayed samples, label for α-CaMKII was aggregated at PSDs in some Purkinje spines (Fig. 6E), but more typically, α-CaMKII label was preferentially located on the sub-PSD spheres (Fig. 6F) or sub-PSD densities. The percentage of total α-CaMKII label associated directly with PSDs in fast-fixed samples did not differ in cerebral and Purkinje spines [24.0% ± 2.8% (n = 34) and 23.2% ± 3.3% (n = 41), respectively]. The increase in α-CaMKII association with PSDs after delayed fixation, however, was significantly lower ($P < 0.0001$) in Purkinje spines [40.3% ± 5.0% (n = 26)] than in cerebral cortical spines [79.7% ± 4.2% (n = 26)].

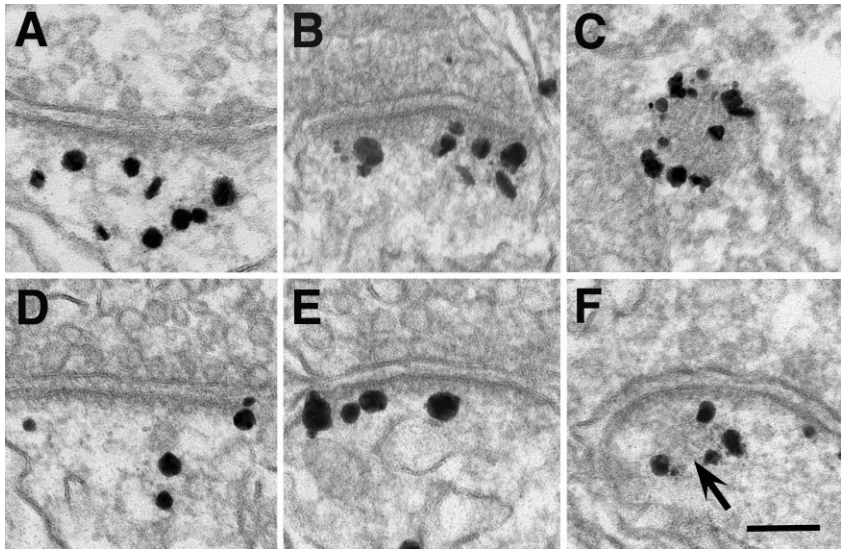

Fig. 6. Label for α-CaMKII (calcium calmodulin-dependent protein kinase II) is dispersed in the spine after fast perfusion fixation in both cerebral (**A**) and cerebellar (**D**) cortices. In cerebrum, after delayed perfusion fixation, α-CaMKII aggregates at the PSD in spines (**B**) and forms clusters in neuronal somas (**C**). In Purkinje spines, α-CaMKII label aggregates either at the PSD (**E**) or at the sub-PSD sphere (**F**, arrow) after delayed perfusion fixation. Scale bar = 0.1 μm.

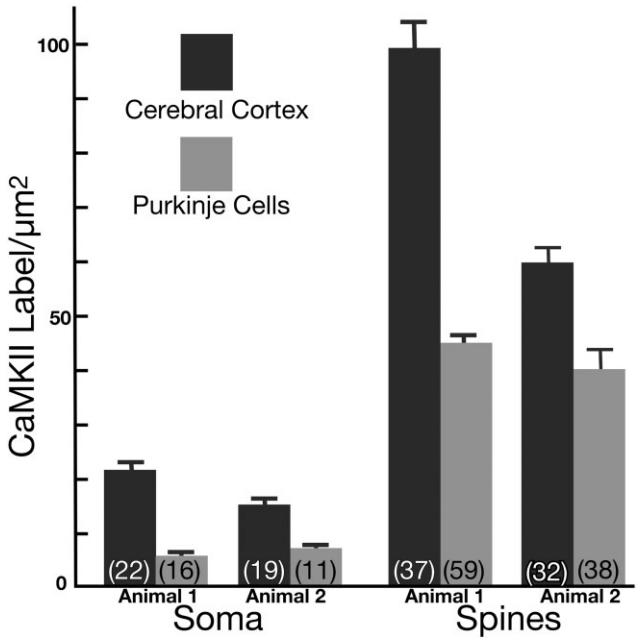

Fig. 7. Density of α-CaMKII label in somas and spines of cerebral and cerebellar cortices after fast perfusion fixation. Parallel data from two animals are shown. Sample size (n) is noted at the base of each bar. Overall lower labeling density in the second animal is attributed to different degrees of fixation and other technical factors.

Effects of delayed perfusion fixation on neuronal somas

Consistent with previous results in rat hippocampus (Tao-Cheng et al., 2001), CaMKII clusters were abundant in neurons from mouse hippocampus and cerebral cortex (α-CaMKII labeled cluster shown in Fig. 6C) after delayed perfusion fixation (Fig. 8B) and absent in fast-fixed samples (Fig. 8A). These cytoplasmic CaMKII clusters are spherical structures (~110 nm in average diameter) presumably composed of densely associated CaMKII molecules (Dosemeci et al., 2000) and often are closely associated with endoplasmic reticulum. As with the smaller sub-PSD CaMKII spheres at Purkinje spines, cytoplasmic CaMKII clusters were apparent, even without immunogold labeling (arrows in Fig. 8B).

CaMKII clusters were encountered much more frequently in forebrain pyramidal cell somas than in Purkinje cells after delayed perfusion fixation. The percentage of somas with cytoplasmic CaMKII clusters was 97% (68 of 70) in hippocampal pyramidal cells and 26% (12 of 46) in Purkinje cells. In somas containing CaMKII clusters, the concentration of clusters was about eight times higher in hippocampal pyramidal cells (0.86 ± 0.05 clusters/μm^2) than in Purkinje cells (0.11 ± 0.02 clusters/μm^2). The degree of CaMKII clustering in neuronal somas appeared to be in step with the concentration of α-CaMKII (Fig. 7).

As in the rat (for review see Takei et al., 1994), mouse cerebellar Purkinje cells showed another striking structural change after delayed perfusion fixation. Endoplasmic reticulum (ER) formed orderly arrays of stacks throughout the Purkinje soma in delay fixed samples (arrowheads in Fig. 8D), but stacks were never seen in fast fixed samples (Fig. 8C). The ability to form massive stacked ER cisternae appears to be characteristic of Purkinje cells, because similar ER stacks were never observed in forebrain pyramidal neuronal somas (Fig. 8A,B). These ER stacks were particularly prominent in Purkinje dendrites near the plasma membrane and sometimes even within spines (Fig. 4D).

DISCUSSION

Here we document artifacts that arise with delay in perfusion fixation of the brain and provide a morphologi-

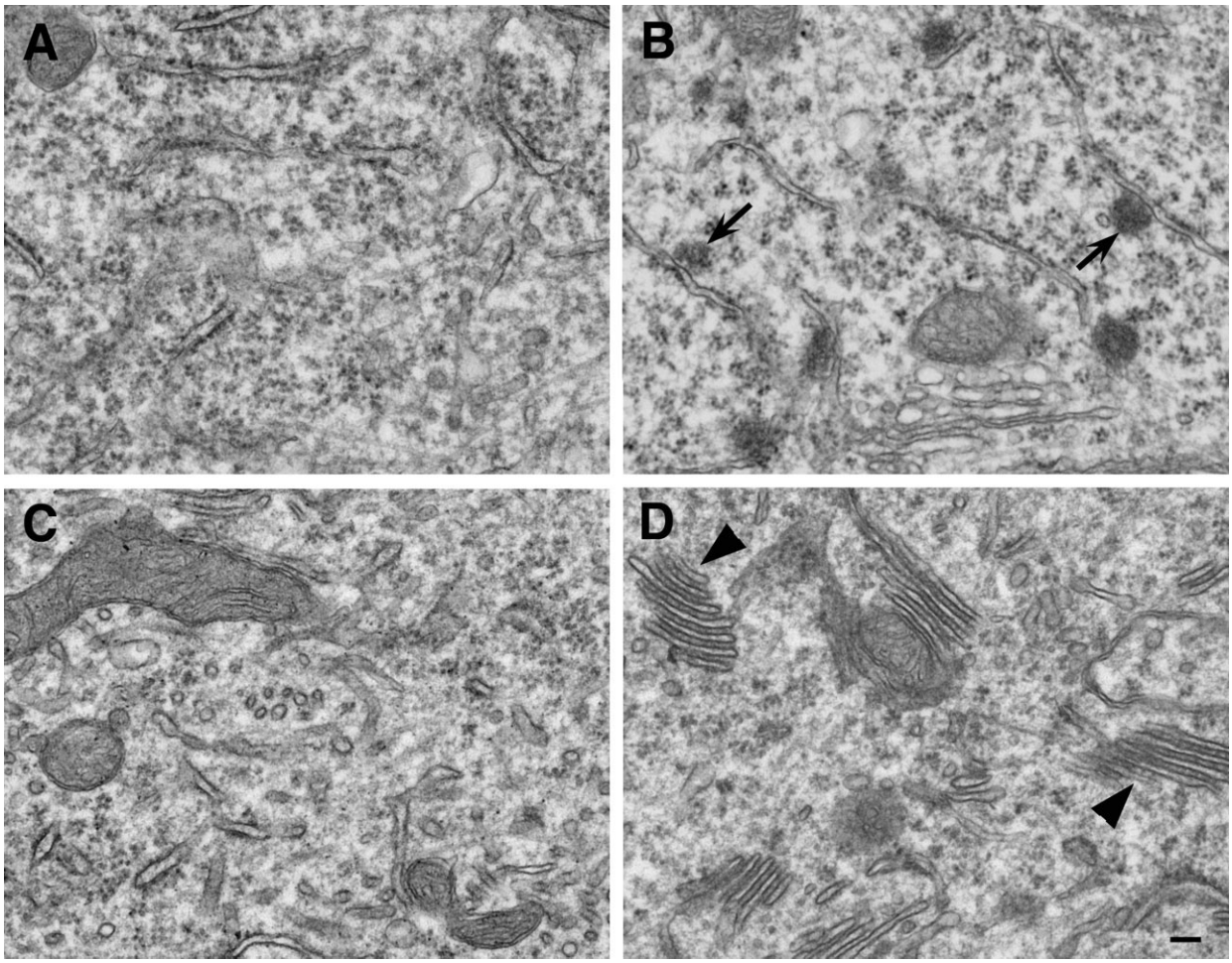

Fig. 8. **A** and **B** compare cerebral cortical pyramidal neuronal somas after fast (A) and delayed (B) perfusion fixations. CaMKII clusters (arrows in B) are abundant after delayed perfusion. **C** and **D** compare cerebellar Purkinje somas after fast (C) and delayed (D) perfusion fixations. Endoplasmic reticulum stacks (arrowheads in D) are prevalent after delayed perfusion fixation. Scale bars = 0.1 μm.

cal baseline for the recognition of changes imposed by experimental manipulations. For delayed fixations, glucose-free physiological saline was perfused through the heart for 5–8 minutes before the fixative was introduced. The gross criteria that we used to select perfusion-fixed samples, depending on hardness and color of perfused brains, effectively eliminated samples that were poorly fixed. Upon EM examination, none of the artifacts typically associated with poor perfusion fixation (Palay et al., 1962; Karlsson and Shultz, 1966) was present in our selected samples. However, even within these well-fixed samples, comparison of delayed- and fast-fixed brains shows that a short delay in perfusion fixation can markedly alter ultrastructure in neurons, especially at synapses.

With delayed perfusion fixation, the PSDs from forebrain synapses become manifestly thicker, accompanied by aggregation of CaMKII at the PSD. These changes are similar to those observed in hippocampal cultures subjected to ischemia-like conditions (Dosemeci et al., 2000). In contrast to the forebrain, PSDs from cerebellar Purkinje spines do not thicken to the same extent or have as much α-CaMKII associated with them after delayed perfusion fixation. In Purkinje spines after delayed perfusion fixation, CaMKII often condensed into sub-PSD spheres ~35 nm away from the PSD, rather than aggregating on the PSD. These sub-PSD spheres are similar in shape and in appearance to the cytoplasmic CaMKII clusters (Dosemeci et al., 2000) but are smaller, 80 nm rather than 110 nm, in average diameter.

Delayed perfusion fixation also results in a significant increase in curvature of the PSD into the synaptic terminals, an increase that is much more prominent in the cerebellar cortex than in the forebrain. Interestingly, the highly curved PSDs often appear in the same Purkinje spines as the sub-PSD CaMKII spheres. Purkinje spines with less curved PSDs sometimes also contain CaMKII-positive sub-PSD densities, but not in a spherical form. These observations suggest a link between the curvature increase and the formation of the 80-nm-sized spheres.

Dense material in the form of multiple spheres lined up beneath the PSD has been described in large dendrites of the frog sympathetic ganglion (Taxi, 1961), cat habenula and interpeduncular nuclei (Milhaud and Pappas, 1966),

and cat spinal cord motor neurons (McLaughlin, 1972), where the PSDs are not highly curved. These structures, called *taxi bodies* or *postsynaptic bodies*, are smaller than the sub-PSD CaMKII spheres reported here. Despite some similarities in appearance, it is not known whether taxi bodies contain CaMKII or whether they are formed in response to the same stimuli as the sub-PSD CaMKII spheres in Purkinje spines. Thus, pending further investigation, the presence of similar sub-PSD dense bodies in any neuronal cell types other than Purkinje cells should not be considered as a sign of delayed perfusion.

Another consequence of delayed perfusion fixation is the appearance of abundant and ordered ER stacks in Purkinje cells. It should be noted that these ER stacks in Purkinje cells are structurally different from the spine apparatus in forebrain synapses, although both entities are composed of stacked membrane cisternae. Spine apparatus is most frequently seen near the base or neck of the spine heads at equal frequency after fast or delayed perfusion fixation. On the other hand, the Purkinje ER stacks contain highly concentrated inositol 1,4,5-trisphosphate receptors (for review see Takei et al., 1994), are specific for Purkinje cells, and are visible throughout the soma and dendrites and in some spines after delayed perfusion fixation. Other conditions that induce the formation of ER stacks in Purkinje cells remain to be investigated.

Our present observation in mouse brains confirms previous work in rat cerebellum (Takei et al., 1994) in which massive ER stacks formed in the Purkinje cells as the result of a few minutes of intracardial perfusion of artificial media preceding fixation. However, despite this cautionary account, flushing out the blood before fixative perfusion has remained a common practice. Our results with fast perfusion fixation demonstrate that, in mice, there is no need to flush out the blood to prevent blood clotting prior to fixative perfusion and that perfusion directly with fixative may prevent dynamic structural changes that might occur during the period of flushing.

The present study also offers reliable benchmarks for screening perfusion-fixed brain samples for signs of delayed fixation at the ultrastructural level. Some consequences of delayed fixation such as PSD thickening in the forebrain and increase in PSD curvature in the cerebellar cortex cannot be conveniently used to detect perfusion delays, because evaluation of such quantitative differences requires meticulous measurements and statistical analysis. On the other hand, certain other structural changes that appear only in delayed-perfusion samples provide more obvious criteria for detecting perfusion fixation delays. These structural changes include formation of cytoplasmic CaMKII clusters in forebrain pyramidal neurons, formation of sub-PSD CaMKII spheres, and appearance of ER stacks in Purkinje cell. We suggest that a simple assessment of these readily discernible structures is sufficient for evaluation of a specimen for perfusion fixation delay in control samples from wild-type animals under resting conditions. The effect of perfusion fixation itself, if not monitored carefully, may mask underlying differences that a study is designed to portray, differences such as structural changes at synapses after genetic or other experimental manipulations. We conclude that comparisons of perfusion-fixed brains from experimental animals are valid only when the control samples are consistently free of any of the signs of perfusion fixation delays.

Although we clearly demonstrate that brief fixation delays produce characteristic structural changes, we do not believe that delayed fixation is the only way to produce these changes. In previous experiments on hippocampal cells in vitro, we demonstrated that metabolic stress (Dosemeci et al., 2000; Tao-Cheng et al., 2001) and N-methyl-D-aspartate (NMDA) stimulation (Dosemeci et al., 2002; Tao-Cheng et al., 2005) produce PSD thickening and cytoplasmic CaMKII clusters. We would predict based on these experiments that any condition that strongly stimulates synaptic activity or produces metabolic stress in vivo might produce structural changes similar to those we report to occur after delayed perfusion fixation. Only when the perfusion fixation is properly controlled, so that the fixation does not itself produce structural changes, will the structural analyses of experimental or pathological conditions be meaningful.

Because perfusion fixation delay is in many respects akin to an ischemic episode, comparison of fast and delayed perfusion fixed samples sheds light on variations in ischemia-induced structural changes in different regions of the brain. Forebrain pyramidal neurons and cerebellar Purkinje cells differ in their response to ischemic stress. In both cells types, CaMKII appears to be involved in many of the observed changes. The concentration of α-CaMKII is approximately two to four times higher (as measured on labeled thin sections) in pyramidal cells than in Purkinje cells. CaMKII clustering by self-association is reported to be a function of the α-subunit (Hudmon et al., 2001), so the lower overall levels of the α-CaMKII in Purkinje cells could explain the deficiency in cytopasmic CaMKII cluster formation in Purkinje cell bodies and processes after delayed perfusion fixation. Indeed, in vitro experiments demonstrate that self-association of CaMKII requires sufficient Ca^{2+} levels and depends on the concentration of CaMKII (Hudmon et al., 2001).

The apparent aggregation of CaMKII in Purkinje spines to form the sub-PSD spheres suggests that, within the confines of these spines, α-CaMKII levels and Ca^{2+} increases can be of sufficient magnitude to support self-association of CaMKII. Purkinje spines indeed had a six- to eightfold higher concentration of α-CaMKII than the soma, a factor in favor of CaMKII self-association. However, even though the forebrain spines have one-and-one-half- to twofold higher levels of α-CaMKII than the Purkinje spines, the CaMKII molecules in forebrain spines invariably aggregate onto the PSD after delayed perfusion fixation, rarely forming sub-PSD aggregates. One explanation for this difference in redistribution of CaMKII in forebrain and Purkinje spines may be the lack of strong or prominent CaMKII binding partners in the Purkinje PSDs. For example, adult Purkinje neurons do not express the NMDA receptor subunit NR2B (Kakegawa et al., 2003), one of the CaMKII-binding proteins (Bayer et al., 2001, 2006), which is abundant in forebrain PSDs.

Because some accumulation of CaMKII does occur in Purkinje PSDs after delayed perfusion fixation, one can assume that CaMKII binding proteins other than NR2B are present in these PSDs. Thus, the amount and type of binding partners in different PSDs might determine whether CaMKII molecules will preferentially bind to the PSD or self-aggregate into sub-PSD spheres in response to ischemic stress. Thus, the relatively small increase in PSD thickening and in PSD-associated CaMKII in Purkinje PSDs compared with forebrain PSDs after delayed fixa-

tion may be due to the overall scarcity of strong CaMKII binding partners in PSDs as well as the lower concentration of CaMKII in Purkinje spines.

ACKNOWLEDGMENTS

We thank Dr. Virginia Pickel for helpful discussions on acrolein perfusion fixation procedures, Dr. Ype Elgersma for helpful discussions, Virginia Crocker and Rita Azzam for EM technical assistance, and John Chludzinski for image processing.

LITERATURE CITED

Bayer KU, De Koninck P, Leonard AS, Hell JW, Schulman H. 2001. Interaction with the NMDA receptor locks CaMKII in an active conformation. Nature 411:801–805.

Bayer KU, LeBel E, McDonald GL, O'Leary H, Schulman H, De Koninck P. 2006. Transition from reversible to persistent binding of CaMKII to postsynaptic sites and NR2B. J Neurosci 26:1164–1174.

Chen X, Vinade L, Leapman RD, Petersen JD, Nakagawa T, Phillips TM, Sheng M, Reese TS. 2005. Mass of the postsynaptic density and enumeration of three key molecules. Proc Natl Acad Sci U S A 102:11551–11556.

Dosemeci A, Reese TS, Petersen J, Tao-Cheng J-H. 2000. A novel particulate form of Ca^{2+}/calmodulin-dependent protein kinase II in neurons. J Neurosci 20:3076–3084.

Dosemeci A, Tao-Cheng J-H, Vinade L, Winters CA, Pozzo-Miller L, Reese TS. 2001. Glutamate-induced transient modification of the postsynaptic density. Proc Natl Acad Sci U S A 98:10428–10432.

Dosemeci A, Vinade L, Winters C, Reese TS, Tao-Cheng J-H. 2002. Inhibition of phosphatase activity prolongs NMDA-induced modification of the postsynaptic density. J Neurocytol 31:605–612.

Erondu NE, Kennedy MB. 1985. Regional distribution of type II Ca^{2+}/calmodulin-dependent protein kinase in rat brain. J Neurosci 5:3270–3277.

Gray EG. 1959. Axo-somatic and axo-dendritic synapses of the cerebral cortex: an electron microscope study. J Anat 93:420–433.

Gundappa-Sulur G, De Schutter E, Bower JM. 1999. Ascending granule cell axon: an important component of cerebellar cortical circuitry. J Comp Neurol 408:580–596.

Hudmon A, Kim SA, Kolb SJ, Stoops JK, Waxham MN. 2001. Light scattering and transmission electron microscopy studies reveal a mechanism for calcium/calmodulin-dependent protein kinase II self-association. J Neurochem 76:1364–1375.

Hudmon A, Lebel E, Roy H, Sik A, Schulman H, Waxham MN, De Koninck P. 2005. A mechanism for Ca^{2+}/calmodulin-dependent protein kinase II clustering at synaptic and nonsynaptic sites based on self-association. J Neurosci 25:6971–6983.

Kakegawa W, Tsuzuki K, Iino M, Ozawa S. 2003. Functional NMDA receptor channels generated by NMDAR2B gene transfer in rat cerebellar Purkinje cells. Eur J Neurosci 17:887–891.

Karlsson U, Schultz RL. 1966. Fixation of the central nervous system for electron microscopy by aldehyde perfusion. J Ultrastruct Res 14:47–63.

Martone ME, Jones YZ, Young SJ, Ellisman MH, Zivin JA, Hu BR. 1999. Modification of postsynaptic densities after transient cerebral ischemia: a quantitative and three-dimensional ultrastructural study. J Neurosci 19:1988–1997.

McLaughlin BJ. 1972. The fine structure of neurons and synapses in the motor nuclei of the cat spinal cord. J Comp Neurol 144:429–460.

Milhaud M, Pappas GD. 1966. Post-synaptic bodies in the habenula and interpeduncular nuclei of the cat. J Cell Biol 30:437–441.

Miller S, Yasuda M, Coats JK, Jones Y, Martone ME, Mayford M. 2002. Disruption of dendritic translation of CaMKIIalpha impairs stabilization of synaptic plasticity and memory consolidation. Neuron 36:507–519.

Palay SL, McGee-Russell SM, Gordon S Jr, Grillo MA. 1962. Fixation of neural tissues for electron microscopy by perfusion with solutions of osmium tetroxide. J Cell Biol 12:385–410.

Peters A, Palay SL. 1996. The morphology of synapses. J Neurocytol 25:687–700.

Peters A, Palay SL, Webste HdF. 1991. The fine structure of the nervous system. New York: Oxford University Press.

Sesack SR, Miner LAH, Omelchenko N. 2006. Pre-embedding immunoelectron microscopy: applications for studies of the nervous system. In: Zaborszky L, Wouterlood FG, Lanciego JL, editors. Neuroanatomical tract-tracing 3: molecules, neurons, systems. New York: Springer. p 6–71.

Silva AJ, Stevens CF, Tonegawa S, Wang Y. 1992. Deficient hippocampal long-term potentiation in alpha-calcium-calmodulin kinase II mutant mice. Science 257:201–206.

Spacek J. 1985. Three-dimensional analysis of dendritic spines. II. Spine apparatus and other cytoplasmic components. Anat Embryol 171:235–243.

Spacek J, Harris KM. 1997. Three-dimensional organization of smooth endoplasmic reticulum in hippocampal CA1 dendrites and dendritic spines of the immature and mature rat. J Neurosci 17:190–203.

Takei K, Mignery GA, Mugnaini E, Sudhof TC, De Camilli P. 1994. Inositol 1,4,5-trisphosphate receptor causes formation of ER cisternal stacks in transfected fibroblasts and in cerebellar Purkinje cells. Neuron 12:327–342.

Tao-Cheng J-H, Vinade L, Smith C, Winters CA, Ward R, Brightman MW, Reese TS, Dosemeci A. 2001. Sustained elevation of calcium induces Ca^{2+}/calmodulin-dependent protein kinase II clusters in neurons. Neuroscience 106:65–74.

Tao-Cheng J-H, Vinade L, Winters CA, Reese TS, Dosemeci A. 2005. Inhibition of phosphatase activity facilitates the formation and maintenance of NMDA-induced CaMKII clusters in hippocampal neurons. Neuroscience 130:651–656.

Taxi J. 1961. [Study of the ultrastkucture of the synaptic zones in the sympathetic ganglia of the frog.] C R Hebd Seances Acad Sci 252:174–176. French.

Walaas SI, Lai Y, Gorelick FS, DeCamilli P, Moretti M, Greengard P. 1988. Cell-specific localization of the alpha-subunit of calcium/calmodulin-dependent protein kinase II in Purkinje cells in rodent cerebellum. Brain Res 464:233–242.